# 2.5D resistivity modeling of embankment dams to assess influence from geometry and material properties

Pontus Sjödahl[1], Torleif Dahlin[1], and Bing Zhou[2]

## ABSTRACT

Repeated resistivity measurement is a potentially powerful method for monitoring development of internal erosion and anomalous seepage in earth embankment dams. This study is part of a project to improve current longterm monitoring routines and data interpretation and increasing the understanding when interpreting existing data. This is accomplished by modeling various occurrences typical of embankment structures using properties from two rockfill embankment dams with central till cores in the north of Sweden. The study evaluates the influence from 3D effects created by specific dam geometry and effects of water level fluctuations in the reservoir. Moreover, a comparison between different layout locations is carried out, and detectability of internal erosion scenarios is estimated through modeling of simulated damage situations. Software was especially developed to model apparent resistivity for geometries and material distributions for embankment dams. The model shows that the 3D effect from the embankment geometry is clearly significant when measuring along dam crests. For dams constructed with a conductive core of fine-grained soil and high-resistive rockfill, the effect becomes greatly enhanced. Also, water level fluctuations have a clear effect on apparent resistivities. Only small differences were found between the investigated arrays. A layout along the top of the crest is optimal for monitoring on existing dams, where intrusive investigations are normally avoided, because it is important to pass the current through the conductive core, which is often the main target of investigation. The investigation technique has proven beneficial for improving monitoring routines and increasing the understanding of results from the ongoing monitoring programs. Although the technique and software are developed for dam modeling, it could be used for estimation of 3D influence on any elongated structure with a 2D cross section.

## INTRODUCTION

Internal erosion is one of the major causes of embankment dam failures. Monitoring systems can significantly improve the safety of such dams. However, to detect erosion early, monitoring systems must be highly sensitive and, at the same time, sufficiently cover the embankment area. In addition, it should be possible to install such monitoring systems in existing dams, and these systems should be capable of identifying small seepage changes, as well as leakage. Experience from research and field installations carried out in Sweden since 1993 indicates that monitoring systems based on resistivity measurements may be able to meet this need (Johansson and Dahlin, 1996; Johansson and Dahlin, 1998; Johansson et al. 2000). In addition, using a resistivity monitoring technique is essentially nondestructive. This is particularly important when working with embankment dams, where drilling and other penetrating investigations are normally avoided.

An electrode layout along the top of the dam core is the most practical and favorable method of installing resistivity monitoring systems on existing dams. This will be shown later in the paper. This method has been shown to be effective in revealing information about conditions in the core itself. In addition, good electrode grounding conditions can be provided in the fine-grained environment commonly found in the dam core (Dahlin et al., 2001). Standard 2D-inversion schemes are a common technique for processing data from resistivity profiling (Smith and Vozoff, 1984; Tripp et al., 1984; Li and Oldenburg, 1992; Loke and Barker, 1995; LaBrecque et al., 1996).

When doing 2D inversion, it is assumed that the properties of the ground are constant in the third dimension, i.e., the direction perpendicular to the electrode layout. Deviations from this are commonly referred to as 3D effects. This means that application of standard 2D techniques on embankment dams with measurement layouts along the crest of the dam cannot be used without cau-

tion because of the obvious 3D effects from the dam geometry. It is possible to use 3D inversion techniques (Park and Van, 1991; Sasaki, 1994; Zhang et al., 1995; Loke and Barker, 1996). However, they still may not be convenient for repeated measurements, mainly because of limitations in computational resources and because data sets are 2D if only measured along the crest. Therefore, a reasonable approach is to use common 2D techniques and then estimate the distortions and errors that are induced in the process. Heretofore, the terms 3D *effect* refer to the errors received when measuring along an embankment, assuming standard 2D conditions. The most obvious effect is the embankment topography; however, the most significant effect might come from the variation in electrical properties of the construction materials in the zoned embankment dam.

The aim of this study was to improve current, longterm monitoring routines on two embankment dams in the north of Sweden. The study covered several situations and scenarios essential for interpreting and evaluating data from resistivity measurements on embankment dams. Investigations of these different situations were carried out through numerical calculations. The influence of the specific dam geometry and zoned construction materials was investigated via dedicated, 2.5D software. Effects of reservoir water level and natural, seasonal resistivity variation in the water were examined as well. Moreover, a comparison was carried out to determine the differences in the efficiency in detecting seepage zones for four different electrode arrays.

Much work has been done on resistivity forward modeling in 2D and 3D using the finite-difference method (Mufti, 1976; Dey and Morrison, 1979a, b; Fox et al., 1980) and the finite-element method (Pridmore et al., 1981; Queralt et al., 1991; Sasaki, 1994; Zhou and Greenhalgh, 2001). Investigative resistivity surveys on embankments to detect structural defects or anomalous seepage are fairly widespread (Abuzeid, 1994; Engelbert et al., 1997; Titov et al., 2000; Van Tuyen et al., 2000; Buselli and Lu, 2001; Panthulu et al., 2001; Voronkov et al., 2004). However, modeling studies to find out more about typical effects from dam geometries is less common.

If 3D modeling were to be used for our study, large and computationally heavy models would have been needed to assess the 3D effects without influence from the finite length of the model. Therefore, software capable of handling typical dam geometries was developed for the numerical calculations. This software is a useful tool for optimizing the monitoring program design and to improve the interpretation of collected data. It uses forward modeling to find the apparent resistivity distribution in earth embankment dams for a given geometry and measurement layout. Additionally, it is general and may be utilized for many types of elongated structures, as long as they can be described with an arbitrary (although constant) geometry in the plane perpendicular to the electrode layout direction.

## NUMERICAL MODELING

### Software description

Software written for 2D resistivity/IP modeling was modified to simulate a dam-monitoring survey by allowing dam geometries in the 2D-model parameterization and a 3D measurement, which means that the current injection and potential pickup may be at any point in the dam. The original 2D software was written for 2D-resistivity tomography and used the common practical situation,

where resistivity tomographic-imaging surveying is conducted in the plane perpendicular to the strike direction, allowing arbitrary variation of resistivity in that plane.

More precisely, the modification of the software was done in two parts. The first considered adjustments of the elements to fit best the outline and the inner structure of the dam (Figure 1), which was done by applying the finite-element method (Zhou, 1998; Zhou and Greenhalgh, 1999). The second part regarded the calculation of the potentials parallel to the strike direction. This was accomplished by performing the inverse, Fourier-cosine transform with nonzero y-coordinate of the potential position, according to the method described by Queralt et al. (1991).

Hence, the modified software is applicable for modeling of the resistivity structure with surface profile or crosshole survey. However, because the current electrodes and the potential measurements must be modeled in 3D for the dam survey, we refer to it as *2.5D modeling*. Assumed resistivities must be constant in the electrode-layout direction, i.e., along the dam, and variable in the dam cross section, whereas the electrodes can be placed anywhere in all three dimensions. Such 2.5D modeling is simply accomplished by involving the inverse Fourier transform for an electrode array parallel to the strike direction (Dey and Morrison, 1979a, b; Queralt et al., 1991). The approach is more efficient than a full 3D model, and for an elongated embankment with constant cross section, the drawbacks are moderate. Hence, it is an efficient tool for assessing 3D effects on 1D and 2D resistivity surveying.

The software uses the finite-element method because this method makes it easier to deal with the dam geometry, compared to the finite-difference method. It is valid for calculating potential, apparent resistivity, or IP responses for a model with arbitrary resistivity distribution in the plane perpendicular to the electrode-layout direction and for any electrode configurations, e.g., surface, crosshole, or *mise-a-la-masse*, off-line and in-line measurements with pole-pole, pole-dipole, dipole-dipole, Schlumberger, and mixed arrays (Zhou and Greenhalgh, 1999).

The accuracy of 2.5D modeling has been checked by comparing it with some known analytic solutions (Zhou, 1998). It has been shown that the modeling accuracy mainly depends on the element size, electrode spacings (that give different ranges of the wavenumber), and the wavenumber sampling (for accurate inverse-Fourier transform). To obtain satisfactory results for the dam modeling, we determined the accuracy-control parameters by applying the dam geometry and the electrode layouts employed in the following simulations. We compared the results with different element sizes and wavenumber sampling schemes. We found that the results showed relative errors less than 1%, using element sizes of about 1 m and 40 wavenumber sampling points.

### Model geometry, material properties, and damage types

The dam model is a zoned embankment dam with a central till core, surrounding filter zones, and support rockfill (Figure 1). This is the most common design of large Swedish embankment dams. Geometry and design values are given in Table 1. The electrode layout is buried 1 m into the top of the core at the midpoint of the cross section.

Because of difficulties in estimating electrical properties of involved materials and lack of appropriate data in literature, some uncertainties are connected to these parameters. Here, the rockfill

was treated as an insulated matrix with all electrical conduction concentrated to the pore spaces. Thus, Archie's law was used using porosity estimates. However, the porosity estimates are to some extent uncertain in themselves. Regarding the core, the matrix can no longer be considered an insulator, and other material models must be used. For this study, the core resistivity was estimated from existing monitoring data from two Swedish dams (Johansson et al., 2000) together with laboratory resistivity measurements of similar till samples (Bergström, 1998) — even though an unsatisfying variation was found in this data.

The resistivity of the filter zones has less influence on the modeling results and was assumed to be somewhere between the resistivity of the core and the rockfill. The resistivity of the reservoir water was taken from monitoring data (Johansson et al., 2000). Electrical material properties are listed in Table 2. In an international perspective, these values are quite high, mainly because of the high resistivity of the water. Assuming a porosity of approximately 25% may lead to resistivities of several thousand ohmmeters in the saturated rockfill. Keep in mind that the main factor influencing the results is the relative differences in resistivities for the involved materials.

The simulated damages were studied for two different depths (Table 3). They could be physically interpreted as damaged layers, possibly resulting from less compaction at initial construction and possibly worsened as a consequence of regional piping causing a transport of fines from the core to the filter and fill. The damages were extended along the full length of the dam. Damaged zones often have this kind of extended shape because the dam is constructed in layers. Even though an extension along the full length of the dam is not realistic, simulating these kinds of scenarios still yields useful information. Furthermore, because of software restrictions, the modeled-dam cross section must be identical along the whole length of the dam. Therefore, for example, it was impossible to simulate a concentrated, cylindrical, damage zone through the dam.

A resistivity increase of five times in the core was assumed because of internal erosion. Experiments on similar tills have shown that resistivity can increase up to 10 times because of removal of fines under water-saturated conditions (Bergström, 1998). However, this should be handled with care because internal erosion increases porosity, affecting the resistivity in the opposite direction. The resistivity of the filter and fill was assumed not to change because of the simulated damages.

## Modeling strategies

To evaluate responses from different electrode arrays, four arrays were selected for all modeling situations. The dipole-dipole, pole-dipole, Wenner-Schlumberger, and gradient arrays were chosen because they have shown robust imaging quality in prior modeling studies (Dahlin and Zhou, 2004). An electrode spacing of 5 m was selected for the dam model because that gives a reasonable relation between electrode spacing and dam height similar to what could be expected in an actual in situ situation. All combinations, including a-spacings from one to seven (multiples of five) and n-factors (one to six), were used for the calculations. The total was 42 individual measurements for each array. Generally, the four different arrays demonstrated similar responses for the different modeled situations. This was particularly true for the pole-dipole, Wenner-Schlumberger, and gradient, which are all geometrically associated. Of the four examined arrays, dipole-dipole is by its nature most different from the others, and in some situations, it gave responses that were different than the others. Thus, only results from dipole-dipole and Wenner-Schlumberger arrays will be presented.

Certainly, when investigating constant cross sections, i.e., no lateral changes, the differences in the design of the arrays will not show up fully in the results. Only when examining special cases, such as cylindrical damages or elongated damage zones with lim-
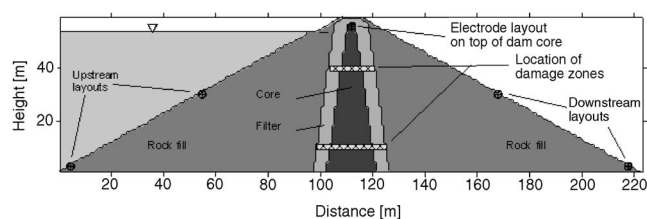


Figure 1. The modeled cross section geometry. A zoned, rockfill embankment dam with a central till core and surrounding filter zones. Electrode layouts and damage zones that are used in the study are marked out.

**Table 1. Dam geometry design parameters (see also Figure 1).**

| | |
|---|---|
| Dam height | 60 m |
| Crest width | 8 m |
| Upstream and downstream slopes | 0.55:1 |
| Distance: Top of core — crest | 3 m |
| Distance: Max reservoir level — crest | 6 m |
| Core width at top/bottom | 4 m/20 m |
| Filter thickness outside core/top core | 4 m/1 m |

**Table 2. Electrical material properties.**

| Material | Resistivity ($\Omega$m) |
|---|---|
| Core | 300 |
| Filter | 2000 |
| Upstream fill | 4000 |
| Downstream fill | 20 000 |
| Reservoir water | 550 |
| Damaged core | 1500 |

**Table 3. Damage types.**

| Damage type | Thickness of damaged layer | Depth from crest to center of damaged layer |
|---|---|---|
| Type 1: Thin seepage zone layer | 2 m | 20 m |
| Type 2: Thin seepage zone layer | 2 m | 50 m |

ited length, can a full verification of the performance of the different arrays be obtained.

## RESULTS

### 3D effects

The 3D effects and their dependency on material parameters were examined for a dam with the model cross section described in Figure 1. The effects were estimated by comparing the responses from two models: a 2.5D model and a 1D model with the properties of the model midsection, i.e., the section with the electrode layout extended to horizontal layers. The 2.5D model generated three to seven times higher responses than the 1D model. Sample results for the dipole-dipole and the Schlumberger arrays are shown in Figure 2.

Next, the dependency of input-material parameters was similarly evaluated using a model with constant resistivity for the whole dam cross section, including the reservoir water. The resulting effect, caused by the topography for a homogeneous embankment, gave an increase in resistivity of about 30% (1.30 times) for the 2.5D model (Figure 3). It is obvious that most of the huge 3D effect arises from the contrast between the relatively conductive core and the high resistivity of the main part of the dam cross section. Most of the current flow is concentrated in the core that geometrically constitutes a rather thin sheet (Figure 4).

### Reservoir-level fluctuations

The effect of lowering the reservoir was examined, using the dam model in Figure 1. This was done because the reservoir water
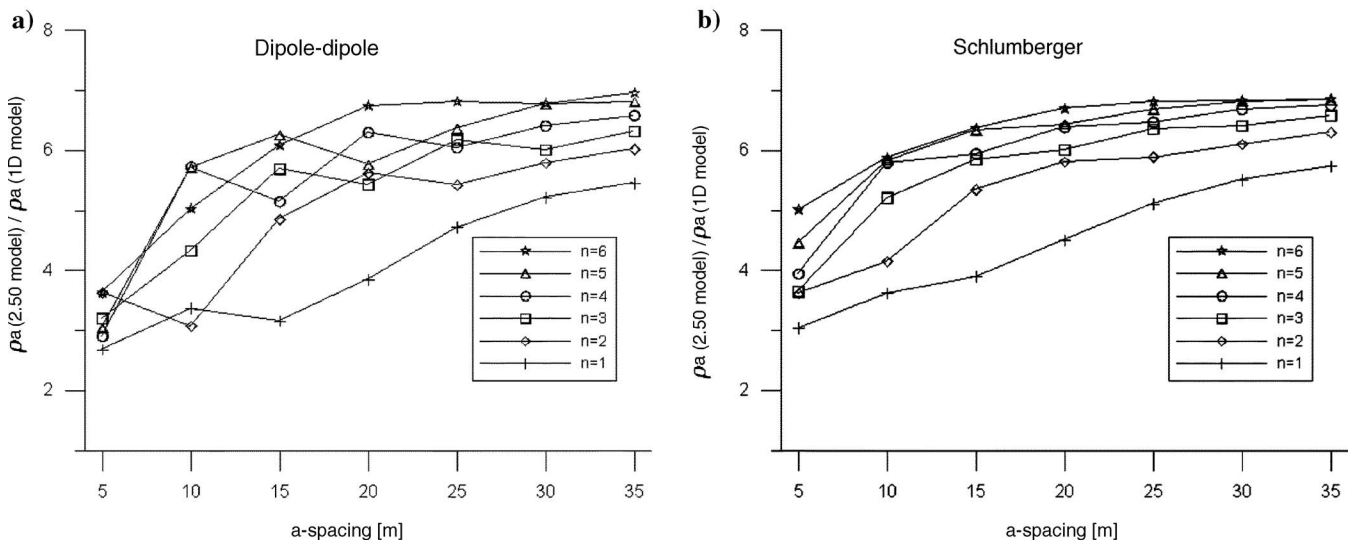


Figure 2. 3D effects estimated as relation between 1D and 2.5D models with assumed material properties for the modeled cross section and reservoir. (a) Dipole-dipole and (b) Wenner-Schlumberger arrays with a-spacing of 5–35 m in steps of 5 m and n-factors 1-6. For both arrays, a-spacing is the spacing between potential electrodes, and n-factor is the shortest distance between potential and current electrode divided by the a-spacing.
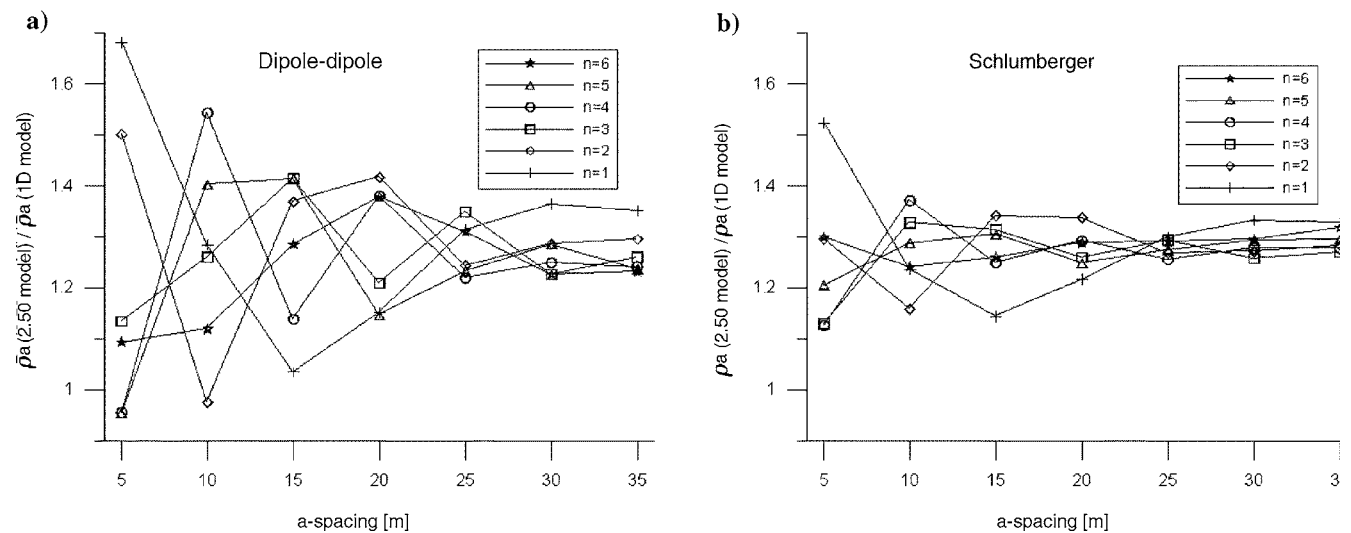


Figure 3. Purely geometrical 3D effects estimated as relation between 1D and 2.5D models with equal material properties in the whole cross section and reservoir. (a) Dipole-dipole and (b) Wenner-Schlumberger arrays with a-spacing of 5–35 m in steps of 5 m and n-factors 1-6.

and its characteristics are the most important factors when monitoring the resistivity inside embankment dams. Two scenarios were investigated: (1) an intermediate lowering of 6 m from full reservoir (from +54 m down to +48 m) and (2) a large lowering of 24 m to almost half of the full depth at +30 m.
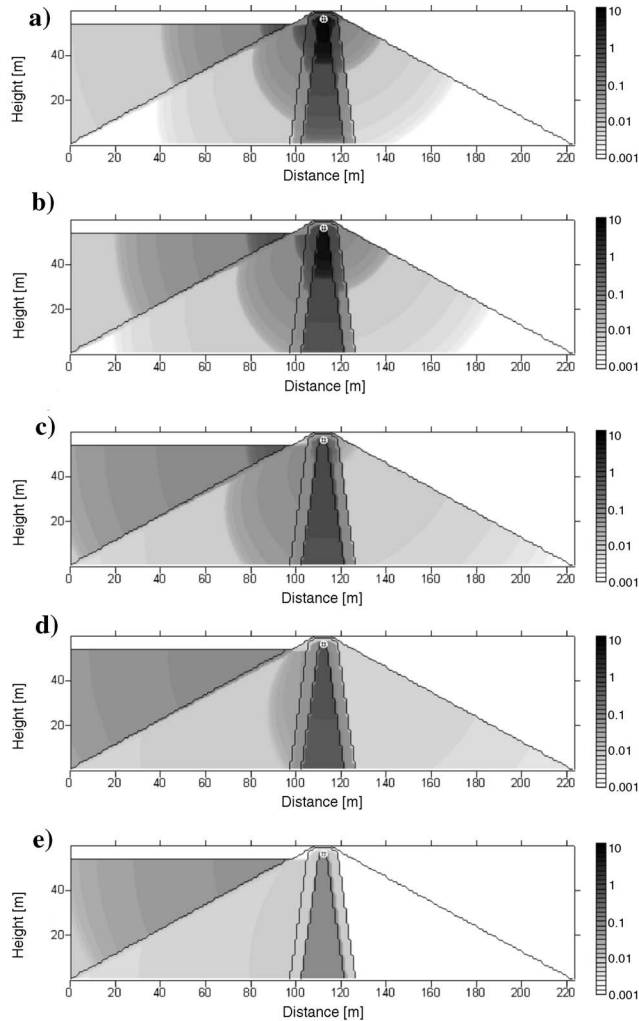


Figure 4. Current density in the cross section in the center between the current electrodes (mA/m² at 1-A transmitted current). Distance between current electrodes increases from (a) 20 m, (b) 40 m, (c) 100 m, (d) 200 m, (e) 400 m.
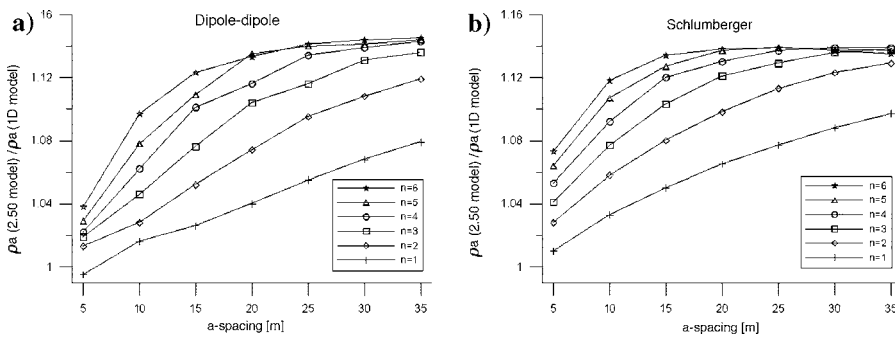


Figure 5. Influence on resistivity measurements along the crest from an intermediate lowering of the reservoir level from maximum level +54 m to + 48 m. (a) Dipole-dipole and (b) Wenner-Schlumberger arrays with a-spacing of 5–35 m in steps of 5 m and n-factors 1-6.

The calculations were made once for each depth. Then, output resistivities were compared with the original, full reservoir model response (Figures 5 and 6). For the intermediate 6-m lowering of the reservoir, a change of close to 14% (1.14 times) was observed for large electrode distances. For the large lowering of the reservoir, the same effect was estimated to be moving toward approximately 40% (1.40 times) for the largest electrode distances.

## Detectability of internal erosion zones

When internal erosion occurs, the material properties of the eroded zone will change as porosity increases and fines are washed away. A permanent or possibly semipermanent change (because it may heal by itself) in the resistivity characteristics of the dam core will occur. To estimate the detectability of such changes, two internal erosion scenarios (Table 3) were set up and modeled using the model described in Figure 1.

The ability to detect the simulated damage types was checked by comparing responses from the leaking model and the ordinary model for each of the four chosen arrays. Anomaly effects from the simulated damage zones were a few percent (1.05–1.07 times) for the damage on large depth (type 2) and more than doubled (1.13–1.17 times) for damage on shallower depth (type 1, Figures 7 and 8).

To estimate the imaging potential of the damages, standard 1D, multilayer, smooth inversion (Auken et al., 2004) was carried out on the forward model responses. The anomaly effect is enhanced through inversion, but effects from the dam geometry cause the damage to localize at a shallower level than the real case (Figure 9).

It is not likely that the damages would be detected by a single survey, but with repeated measurements the possibilities would be fair. The negative anomaly effect at larger depths is most likely an effect from inversion that would probably disappear when using time-lapse inversion.

## Comparison of different layout locations

Modeling of different layout placements is helpful for interpreting data from Swedish dam monitoring, especially at the Hällby Dam, where layouts are not only placed along the crest but also on a line along the upstream and the downstream side (Johansson et al., 2000). The standard model (Figure 1) was used, together with each of the simulated damage zones described in Table 3, and the anomaly effect was calculated for four different placements of the layouts. These placements were the upstream toe, the mid-upstream slope, the mid-downstream slope, and the downstream toe. All of them are placed directly beneath the surface of the dam. Consequently, for the layouts along the upstream toe and the mid-upstream slope, the upstream electrodes are placed below the water table.

The modeling results demonstrate that the four alternative layout placements are clearly inappropriate in detecting changes inside the core. The calculated-anomaly effects are less than 1% (<1.01 times) for all different placements of the layouts, re-
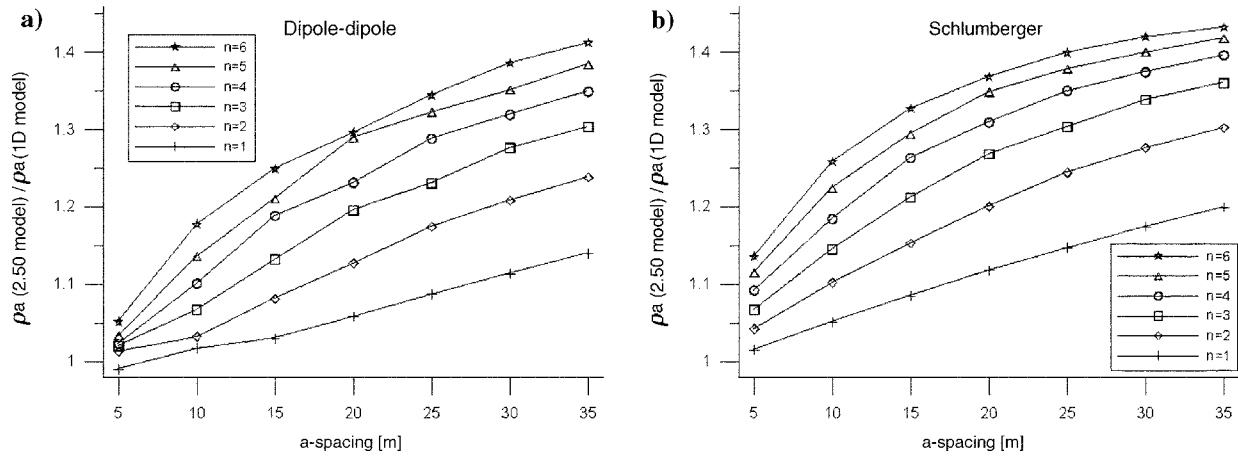
Figure 6. Influence on resistivity measurements along the crest from a large lowering of the reservoir level from maximum level +54 m to + 30 m. (a) Dipole-dipole and (b) Wenner-Schlumberger arrays with a-spacing of 5–35 m in steps of 5 m and n-factors 1-6. For both arrays, a-spacing is the spacing between potential electrodes and n-factor the shortest distance between potential and current electrode divided by the a-spacing.
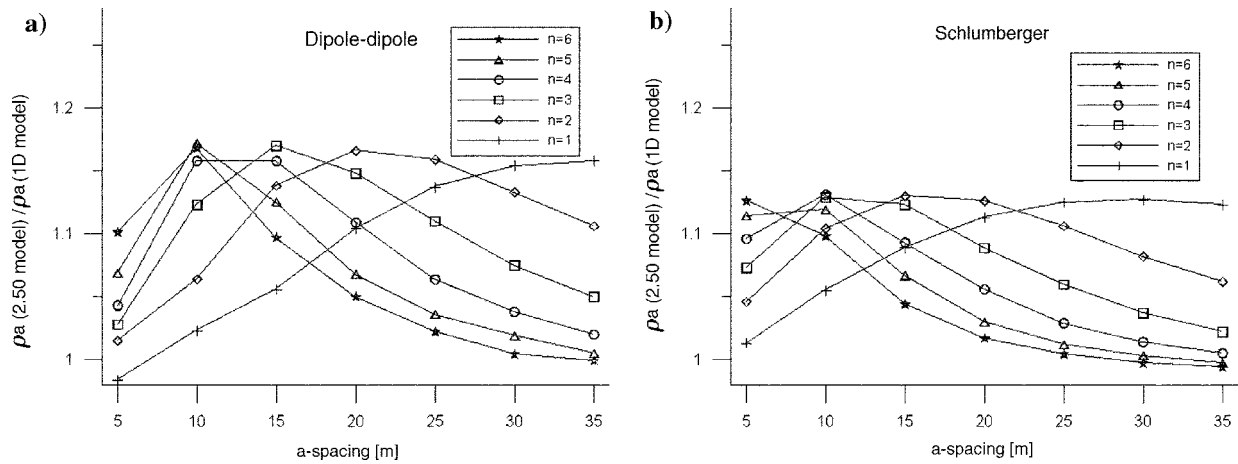


Figure 7. Anomaly effect from damage type 1 expressed as relation in apparent resistivities between the leaking model and the ordinary model. (a) Dipole-dipole and (b) Wenner-Schlumberger arrays with a-spacing of 5–35 m in steps of 5 m and n-factors 1-6. For both arrays, a-spacing is the spacing between potential electrodes and n-factor is the shortest distance between potential and current electrode divided by the a-spacing.
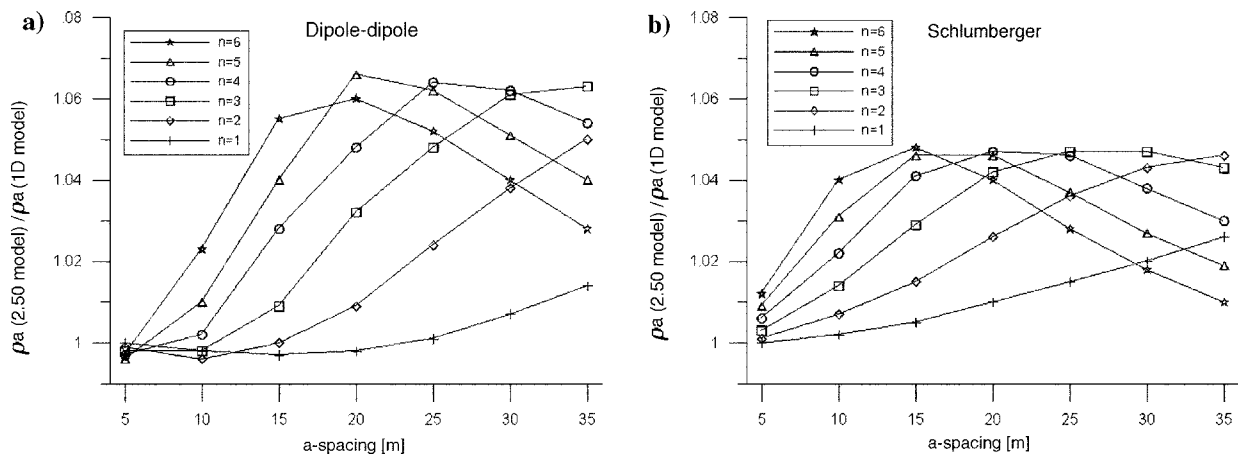


Figure 8. Anomaly effect from damage type 2 expressed as relation in apparent resistivities between the leaking model and the ordinary model. (a) Dipole-dipole and (b) Wenner-Schlumberger arrays with a-spacing of 5–35 m in steps of 5 m and n-factors 1-6.
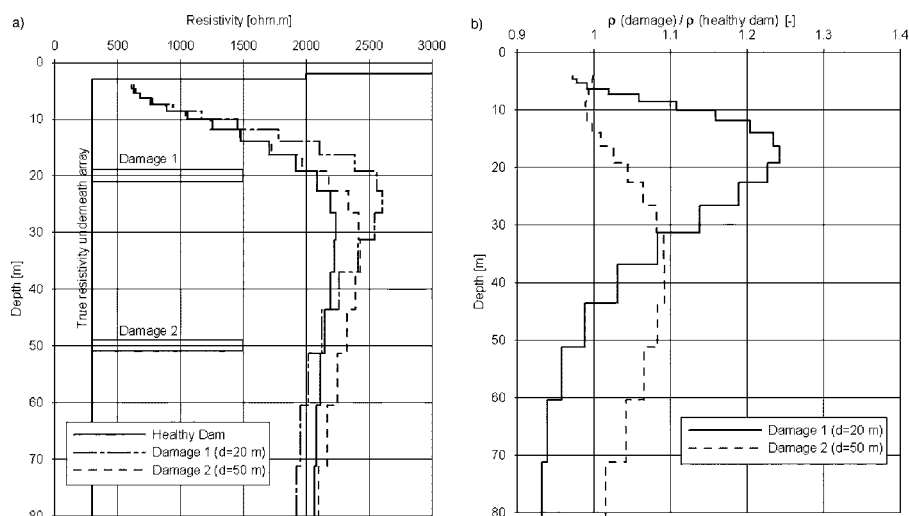
Figure 9. (a) Model resistivities and (b) anomaly effects expressed as the ratio between damaged and healthy dam for damage types 1 and 2, using standard 1D, multilayer, smooth inversion of data from Wenner-Schlumberger array generated by the forward model. The array is located at 4 m depth along the top of the dam core.

gardless of the damage location. This must be regarded as clearly unsatisfactory, considering the size of the damage and that a layout along the top of the core produces a clearly superior anomaly effect: 1.13–1.17 times for damage type 1 and 1.05–1.07 times for damage type 2.

Obviously, the channeling effect that concentrates current flow within the conductive dam core is an important factor. However, in a real situation, a possible internal erosion scenario also might induce other effects that could be detectable for these layouts; for instance, an increased, concentrated seepage below the foundation level of the downstream toe with associated temperature-induced resistivity variation. In this case, only a spatially limited change within the dam core was assumed.

## DISCUSSION AND CONCLUSIONS

Resistivity measurements on embankment dam geometries are influenced by many factors, such as effects caused by the geometry and variation in material properties across the dam cross section, impact of water-level changes, and electrode-layout location. Forward resistivity modeling was used to estimate the sensitivity of geoelectrical measurements to changes in the mentioned factors. An efficient way of carrying out the study is a 2.5D approach, where the only restriction, compared to a full-3D model, is a constant dam cross section.

This study shows that the 3D effect arising from dam geometry has a strong influence on the measured resistivity of the dam structure when the electrode layout is located along the dam crest. The influence is similar for all of the examined arrays, ranging from three to seven times the value of the standard 1D model for the geometry and material properties assumed. The 2D surveys with the electrode layout along the dam crest will respond in the same way. Furthermore, the 3D effect generally increases with increasing current-electrode distances. This can be expected when a larger earth body is involved. The modeling results are heavily dependent on the electrical properties of the materials, and additional efforts

will be undertaken to make more precise estimations of these properties. However, even with a constant resistivity of the whole dam cross section, the effect caused by the topography is significant (about 30%). The strong 3D effect also means that much of the current is concentrated in the conductive dam core — a fact that enhances the possibilities to detect damage in the core with electrode layouts along the dam crest.

It is well known that reservoir characteristics govern the resistivity variation pattern inside the dam. Reservoir elevation and resistivity of reservoir water are therefore crucial to interpret resistivity data from dam-crest measurements. Resistivities measured along the dam crest were shown to be significantly influenced by fluctuations in the reservoir level. A drop in the reservoir level from 54 m to 48 m resulted in a change in measured resistivity of up to 14%. For the larger lowering of the reservoir down to 30 m, the resistivity was affected by about 40%. The effect from lowering the reservoir is in the same order of magnitude or higher than could be expected from a damage zone. Therefore, it is essential to track and compensate for such effects when evaluating resistivity data from embankment dams.

Modeling of leaky structures was carried out. Limitations of the software made it impossible to evaluate damages with limited extension along the dam. Even though weak zones in dams often have a layered shape, such elongated damages are not realistic. At this point, these damages still give us a rough estimate of what kind of detection possibilities to expect. Anomaly effects from the simulated damage zones were shown to range from a few percent for damage type 2 to approximately 15% for damage type 1. It is unlikely that such damages could be detected by a single resistivity survey using surface electrodes. In case of repeated measurements or regular monitoring, however, detection possibilities would be promising.

Dipole-dipole has proved to give the largest anomaly effect for all of the damage types, whereas the others gave slightly lower, but similar, responses. However, because the dipole-dipole array from earlier studies has proved to be most sensitive to noise (Zhou and Dahlin, 2003), it may not be the optimal array in practical application. Also note that all damage types were shaped as extended layers and that the results may not be fully applicable, for instance, to a cylindrically shaped damage and other damage zones with limited extent along the dam. Such investigations require using a full 3D model approach.

## ACKNOWLEDGMENTS

## REFERENCES

Abuzeid, N., 1994, Investigation of channel seepage areas at the existing Kaffrein dam site (Jordan) using electrical-resistivity measurements: Journal of Applied Geophysics, **32**, 163–175.

Auken, E., A. V. Christiansen, B. H. Jacobsen, N Foged, and K. I. Sørensen, 2004, Piecewise 1D laterally constrained inversion of resistivity data: Geophysical Prospecting, **53**, 497–506.

Bergström, J., 1998, Geophysical methods for investigating and monitoring the integrity of sealing layers on mining waste deposits: Licentiate Thesis, Luleå University of Technology.

Buselli, G., and K. Lu, 2001, Groundwater contamination monitoring with multichannel electrical and electromagnetic methods: Journal of Applied Geophysics, **48**, 11–23.

Dahlin, T., P. Sjödahl, J. Friborg, and S. Johansson, 2001, Resistivity and SP surveying and monitoring at the Sädva Embankment Dam, Sweden: Presented at the 5th European International Commission in Large Dams Symposium, 107–113.

Dahlin, T., and B. Zhou, 2004, A numerical comparison of 2D resistivity imaging with ten electrode arrays: Geophysical Prospecting, **52**, 379–398.

Dey, A., and H. F. Morrison, 1979a, Resistivity modeling for arbitrarily shaped two-dimensional structure: Geophysical Prospecting, **27**, 106–136.

——, 1979b, Resistivity modeling for arbitrarily shaped three-dimensional structure: Geophysics, **44**, 753–780.

Engelbert, P. J., R. H. Hotchkiss, and W. E. Kelly, 1997, Integrated remote sensing and geophysical techniques for locating canal seepage in Nebraska: Journal of Applied Geophysics, **38**, 143–154.

Fox, R. C., G. W. Hohmann, T. J. Killpack, and L. Rijo, 1980, Topographic effects in resistivity and induced-polarization surveys: Geophysics, **45**, 75–93.

Johansson, S., and T. Dahlin, 1996, Seepage monitoring in an earth embankment dam by repeated resistivity measurements: European Journal of Engineering and Environmental Geophysics, **1**, 229–247.

——, 1998, Seepage monitoring in Hällby embankment dam by continuous resistivity measurements: Presented at the 8th Congress of the International Association of Engineering Geology and the Environment.

Johansson, S., T. Dahlin, and J. Friborg, 2000, Seepage monitoring by resistivity and streaming potential measurements at Hällby Embankment Dam 1996–1999, Report 00:15, Elforsk, Stockholm.

LaBrecque, D., M. Miletto, W. Daily, A. Ramirez, and E. Owen, 1996, The effects of noise on Occam's inversion of resistivity tomography data: Geophysics, **61**, 538–548.

Li, Y. G., and D. W. Oldenburg, 1992, Approximate inverse mapping in DC resistivity problems: Geophysical Journal International, **109**, 343–362.

Loke, M. H., and R. D. Barker, 1995, Least-squares deconvolution of apparent resistivity pseudosections, Geophysics, **60**, 1682–1690.

——, 1996, Practical techniques for 3D resistivity surveys and data inversion: Geophysical Prospecting, **44**, 449–523.

Mufti, I. R., 1976, Finite difference resistivity modeling for arbitrary shaped two-dimensional structures: Geophysics, **41**, 62–78.

Panthulu, T. V., C. Krishnaiah, and J. M. Shirke, 2001, Detection of seepage paths in earth dams using self-potential and electrical resistivity methods: Engineering Geology, **59**, 281–295.

Park, S. K., and G. P. Van, 1991, Inversion of pole-pole data for 3-D resistivity structure beneath arrays of electrodes: Geophysics, **56**, 951–960.

Pridmore, D., G. W. Hohmann, S. H. Ward, and W. R. Sill, 1981, An investigation of finite element modeling for electrical and electromagnetic modeling data in three dimensions: Geophysics, **46**, 1009–1024.

Queralt, P., J. Pous, and A. Marcuello, 1991, 2-D resistivity modeling: An approach to arrays parallel to the strike direction: Geophysics, **56**, 941–950.

Sasaki, Y., 1994, 3-D resistivity inversion using the finite element method: Geophysics, **59**, 1839–1848.

Smith, N. C., and K. Vozoff, 1984, Two-dimensional DC resistivity inversion for dipole-dipole data: IEEE Transactions Geoscience and Remote Sensing, **GE-22**, 21–28.

Titov, K., V. Lokhmanov, and A. Potapov, 2000, Monitoring of water seepage from a reservoir using resistivity and self polarization methods: Case history of the Petergoph fountain water supply system: First Break, **18**, 431–435.

Tripp, A. C., G. W. Hohmann, and C. M. Swift, Jr., 1984, Two-dimensional resistivity inversion: Geophysics, **4**,9, 1708–1717.

Van Tuyen, D., T. Canh, and A. Weller, 2000, Geophysical investigations of river dikes in Vietnam: European Journal of Environmental and Engineering Geophysics, **4**, 195–206.

O. K. Voronkov, A. A. Kagan, N. F. Krivonogova, V. B. Glagovsky, and V. S. Prokopovich, 2004, Geophysical methods and identification of embankment dam parameters, Proceedings of the 2nd International Conference on Site Characterization (ISC-2), 593–599.

Zhang, J., R. Mackie, and T. Madden, 1995, 3-D resistivity forward modeling and inversion using conjugate gradients: Geophysics, **60**, 1313–1325.

Zhou, B., 1998, Crosshole resistivity and acoustic velocity imaging, in 2.5-D Helmholtz equation modeling and inversion: Ph.D. thesis, The University of Adelaide.

Zhou, B., and T. Dahlin, 2003, Properties and effects of measurement errors on 2D resistivity imaging surveying: Near Surface Geophysics, **1**(3), 105–117.

Zhou, B., and S. A. Greenhalgh, 1999, Explicit expressions and numerical calculations for the Fréchet and second derivatives in the 2.5D Helmholz equation inversion: Geophysical Prospecting, **47**, 443–468.

——, 2001, Finite element three-dimensional direct current resistivity modeling: Accuracy and efficiency considerations: Geophysical Journal International, **145**, 679–688.